J. Moll. Stud. (2000), **66**, 457–466

REMOTE BIOMINERALIZATION IN DIVARICATE RIBS OF *STRIGILLA* AND *SOLECURTUS* (TELLINOIDEA: BIVALVIA)

ANTONIO G. CHECA
Departamento de Estratigrafía y Paleontología, Facultad de Ciencias, Universidad de Granada, 18071 Granada, Spain [acheca@goliat.ugr.es]
(Received 22 November 1999; accepted 20 February 2000)

ABSTRACT

Deposits composed of aragonite prisms, which were formed after the outer shell layer, have been found at the posterior steep slopes of divaricate ribs in two species of *Strigilla* and another two of *Solecurtus*. These prisms have their axes oriented perpendicular to the outer shell surface and differ in morphology from fibres of the surface-parallel composite prisms forming the outer shell. They display crystalline features indicating that, unlike crystals forming the outer shell surface, their growth front was free, unconstrained by the mantle or periostracum. These particular deposits are called free-growing prisms (FGPs). In these genera the periostracum is clearly not the substrate for biomineralization and, upon formation, does not adhere to the steep slope of ribs, but detaches at the rib peak and reattaches towards the posterior, just beyond the foot of the posterior scarps of ribs. In this way, a sinus or open space developed between the internal surface of the periostracum and the outer shell surface along each steep rib slope. These spaces could remain filled with extrapallial fluid after the mantle advances beyond that point during shell secretion. FGPs grow within this microenvironment, out of contact with the mantle. Other species with divaricate ribs do not develop FGPs simply because the periostracum adheres tightly to both rib slopes (which are never so steep as in *Solecurtus* and *Strigilla*). FGPs constitute one of the rare cases of remote biomineralization in which aragonite is produced and direct contact with the mantle never takes place.

INTRODUCTION

Present-day models for shell biomineralization in bivalves imply the presence of the mantle as an essential element in calcification (e.g., Crenshaw, 1980; Wilbur & Saleuddin, 1983; Lowenstam & Weiner, 1989, and references therein). During shell secretion, ions (Ca^{2+}, HCO_3^-) and organic components are released by the mantle into the extrapallial space, which becomes the microenvironment of shell deposition. Chinzei & Seilacher (1993) showed the presence of a varied array of calcite deposits in the cavities between shell layers left by the mantle in the attached valve of several ostreoids. These authors convincingly interpreted these structures as having formed after closure of the chambers. They used the term 'remote biomineralization' to denote processes in shells without direct influence from living tissue. Other examples studied in recent and fossil cephalopods (Seilacher & Chinzei, 1993) differ in that the mantle or siphuncular tissue at some stage made contact with the deposit. Kemperman & Gittenberger (1988) illustrated crystalline deposits of aragonite and, possibly, vaterite (J.M. García-Ruiz, personal communication) within the hollow ribs of Clausiliidae (Gastropoda), which represent a unique case of remote biomineralization.

During research on the formation of divaricate and other kinds of oblique ribs of bivalves, we found particular deposits of aragonite occurring at the steep slopes of divaricate ribs of some species of the tellinoidean genera *Strigilla* and *Solecurtus*. Their appearance and distribution suggest that they form independently from the rest of the shell. Here we interpret these deposits as a particular case of remote biomineralization. Their inferred mode of formation provides insight into the morphodynamics of divaricate ribs in these genera.

MATERIAL AND TECHNIQUES

The above mentioned crystalline deposits were found only in the Tellinidae *Strigilla polyaulax* Tomlin & Shackelford and *S. pisiformis*, (Linnaeus) and in the Psammobiidae *Solecurtus strigilatus* (Linnaeus) and *S. philippinensis* Dunker, from a larger sample of species with divaricate or oblique ribs. All the material examined is listed in Table 1.

Variously prepared samples were examined by SEM in a Zeiss DSM 950. Intact samples of the above

Table 1. Details of taxa and specimens investigated, with indication of the occurrence of FGPs. unreg. = unregistered; pv = paired valves; uv = loose valves; lv = left valve; rv = right valve; MNHN = Muséum National d'Histoire Naturelle, Paris; MNCN = Museo Nacional de Ciencias Naturales, Madrid; SPUGR = Departamento de Estratigrafía y Paleontología, Universidad de Granada. All the material is Recent, except for *Myllita* sp. (Pliocene).

Taxon	Locality	Material/SEM specimens	FGPs
Nuculoida			
Acila fultoni Smith 1892	Bengal Bay, India	16 pv (MNHN, unreg.)/1 rv	No
Acila sp.	Philippines	10 pv (MNHN, unreg.)/1 lv	No
Nuculana bicuspidata Gould, 1845	Senegal	4 pv (SPUG.BV.102-103)/1 lv	?
Heterodonta			
Divaricella dentata (Wood, 1815)	Florida Keys	32 uv (MNHN, unreg.)/1 lv + 1 rv	No
Divaricella quadrisulcata (Orbigny, 1842)	Isla Mujeres, Mexico	5 uv (SPUG.BV.94-98)/1 lv + 1 rv No	
Divaricella gibba (Gray, 1825)	Port Gentil, Gabon	4 uv (MNHN, unreg.)/1 rv	No
Divalucina cumingi (Adams & Angas, 1863)	a. South Natal, South Africa	a. 37 uv (MNHN, unreg.)/1 rv	No
	b. Unknown	b. 4 pv (MNHN, unreg.)	
Myllita sp,	Málaga, Spain	5 uv (SPUG.BV.503-507)/1 rv	No
Digitaria digitaria (Linnaeus, 1758)	Málaga, Spain	14 pv (SPUG.BV.62-68)/2 lv + 1 lv	No
Strigilla polyaulax Tomlin & Shackelford, 1915	a. Pointe Noire, Congo Brazzaville	a. 4 pv (SPUG.BV.202-203)/2 rv + 1 lv	Yes
	b. Luanda, Angola	b. 2 pv (SPUG.BV.204)/1 rv + 1 lv	
Strigilla carnaria (Linnaeus, 1758)	Caribbean	10 pv + 1 uv (MNHN, unreg.)/1 lv	?
Strigilla pisiformis (Linnaeus, 1758)	Caribbean	23 uv (MNHN, unreg.)/1 lv + 1 rv	Yes
Gari maculosa (Lamarck, 1818)	a. Philippines	a. 8 pv (MNCN, 15.07/0005, 15.07.0013, 15.07/0035)/1 rv	No
	b. Philippines	b. 6 pv (MNHN, unreg.)/1 lv	
Gari squamosa (Lamarck, 1818)	Philippines	20 pv + 1 uv (MNCN, 15.07/0003, 15.07/0142)/1 rv	No
Solecurtus strigilatus (Linnaeus, 1758)	Almeria, Spain	8 pv (SPUG.BV.142-145)/1 lv + 2 rv	Yes
Solecurtus philippinensis Dunker, 1861	Luzón, Philippines	18 pv (MNCN, 15.07/4768)/1 lv	Yes

species, with and without periostracum (removed with sodium hypochlorite) were used to discern surface features. Radially fractured valves (slightly etched in 1% hydrochloric acid) of the species of *Solecurtus* and *Strigilla* were also examined. Finally, some shell pieces of *S. strigilatus* and *S. polyaulax* were embedded in epoxy resin, cut radially, ground and etched.

Calcium carbonate polymorphs were determined by both crystal morphology and immersion in Feigl's (1937) solution, in which aragonite stains black in a matter of minutes, whereas calcite needs a much longer time.

GENERAL SHELL FEATURES

Strigilla species display thin and closely spaced ribs, which have both a radial and posterior growth component in the central area of the shell. In *S. pisiformis*, there is a posterior and an anterior bifurcation radial line (Fig. 1A), while in *S. polyaulax* the anterior shell sector contains purely commarginal ribs. In the much larger specimens of *Solecurtus*, ribs are directed anteriorly and the bifurcation line is placed more (*S. philippinensis*) or less (*S. strigilatus*; Fig. 1B) anteriorly. The anteriormost area is unsculptured.

Ribs are invariably asymmetric in profile with an abrupt, almost vertical posterior face and a gentle anterior slope. This feature is related to their main burrowing-enhancing function (Stanley, 1970; Seilacher, 1972).

In both genera the aragonitic shell has a thin outer denticular composite prismatic layer, in which the long axes of prisms are parallel to the shell surface (Figs. 2F & 3G). Measured thicknesses vary from 20–40 μm in *Solecurtus* and 60–100 μm in *Strigilla*. The underlying layer is crossed-lamellar, with lamellae running trans-

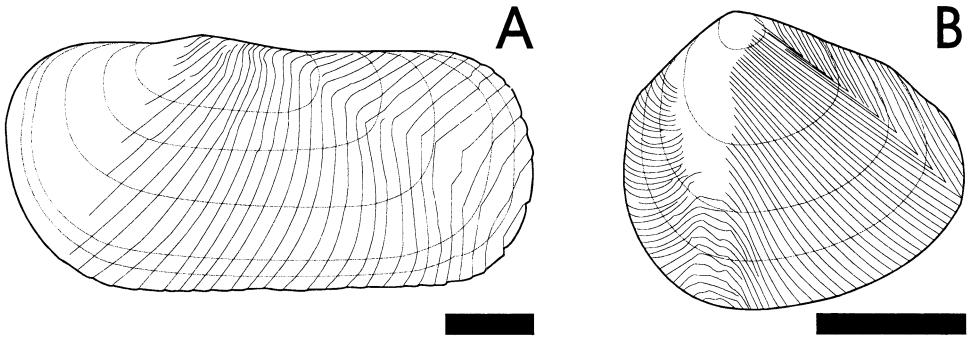

Figure 1. Schematic distribution of ribs on the left valves of (**A**) *Solecurtus strigilatus* and (**B**) *Strigilla carnaria*. The steep slope of ribs consistently faces in a posterior direction. Scale bar (= 1 cm) gives an approximate idea of the relative sizes of adult shells.

verse to the growth surface in both genera. This distribution of shell layers agrees completely with the one described for *S. strigilatus* and other tellinoideans by Taylor, Kennedy & Hall (1973, Table 10). According to these authors there is an innermost layer, behind the pallial line (complex crossed-lamellar in *S. strigilatus*), which we have not examined.

The periostracum was well preserved in live-taken specimens of *Solecurtus* (Fig. 2A), especially towards the most recently secreted part of the shell. Tiny periostracal remains were observed under SEM in *S. polyaulax*, but were absent in the specimens (apparently all taken stranded) of the other species.

LOCATION AND DESCRIPTION OF FREE-GROWING PRISMS (FGPs) IN *STRIGILLA AND* SOLECURTUS

Shell surfaces have a polished appearance when viewed by SEM, except for the low relief of the boundaries between composite prisms in *Solecurtus* (Fig. 2B). Only when going from the gentle to the steep slopes of ribs in an anterior direction does the shell become rougher in appearance (Figs. 2B, C & 3A, D). This is caused by deposits consisting of prismatic crystals which are markedly coarser than the fibres of the underlying prisms (Fig. 2F, G, H & 3H). These crystals grow perpendicular to the shell surface, reach irregular heights and display clear crystalline endings (Figs. 2E & 3C). This pattern indicates that their growth front was free and not limited by a common mantle or periostracum surface, contrary to what is usual in the bivalve shell. On the basis of this character, we will call them free-growing prisms (FGPs).

In *Solecurtus*, FGPs display typical pseudohexagonal transverse sections (Fig. 2D, E), which reflects polysynthetic twinning of aragonite crystals (J.M. García-Ruiz, personal communication). The aragonitic nature of FGPs is also revealed by their higher degree of staining than the rest of the aragonitic shell after immersion in Feigl's solution for 20 minutes. FGPs are perpendicular to the shell surface in transversal section, but they show a marked change in orientation with respect to the (more horizontal) fibres of the underlying prisms (Fig. 2F, G, H). They differ also in being several times wider (1–2 μm wide) compared to lesser units of prisms (Fig. 2D, G, H). These deposits also line the grooves provided by the boundaries between prisms growing adjacent to the ribs, which apparently do not completely close off the volume underlying the periostracum (Fig. 2C). Some growth lines originating at the lowest part of the step and vanishing posteriorwards are also composed of this kind of material (Fig. 2B).

In *Strigilla*, FGPs are also found at the steep posterior slopes of ventral ribs (Fig. 3A, B, D), but neither at the posterior nor the anterior ribs. The arrangement of crystals is very similar to that of *Solecurtus*. The growing edge of the shell of *Strigilla* strongly reflects backwards to become almost parallel to the outer surface of the shell (Fig. 3E, G), which causes the fibres of the horizontal composite prisms to become perpendicular to the shell surface. FGPs grow with the same orientation, extending the fibres of the prisms (from which they differ in being larger, 1–3 μm wide) (Fig. 3H). In surface view,

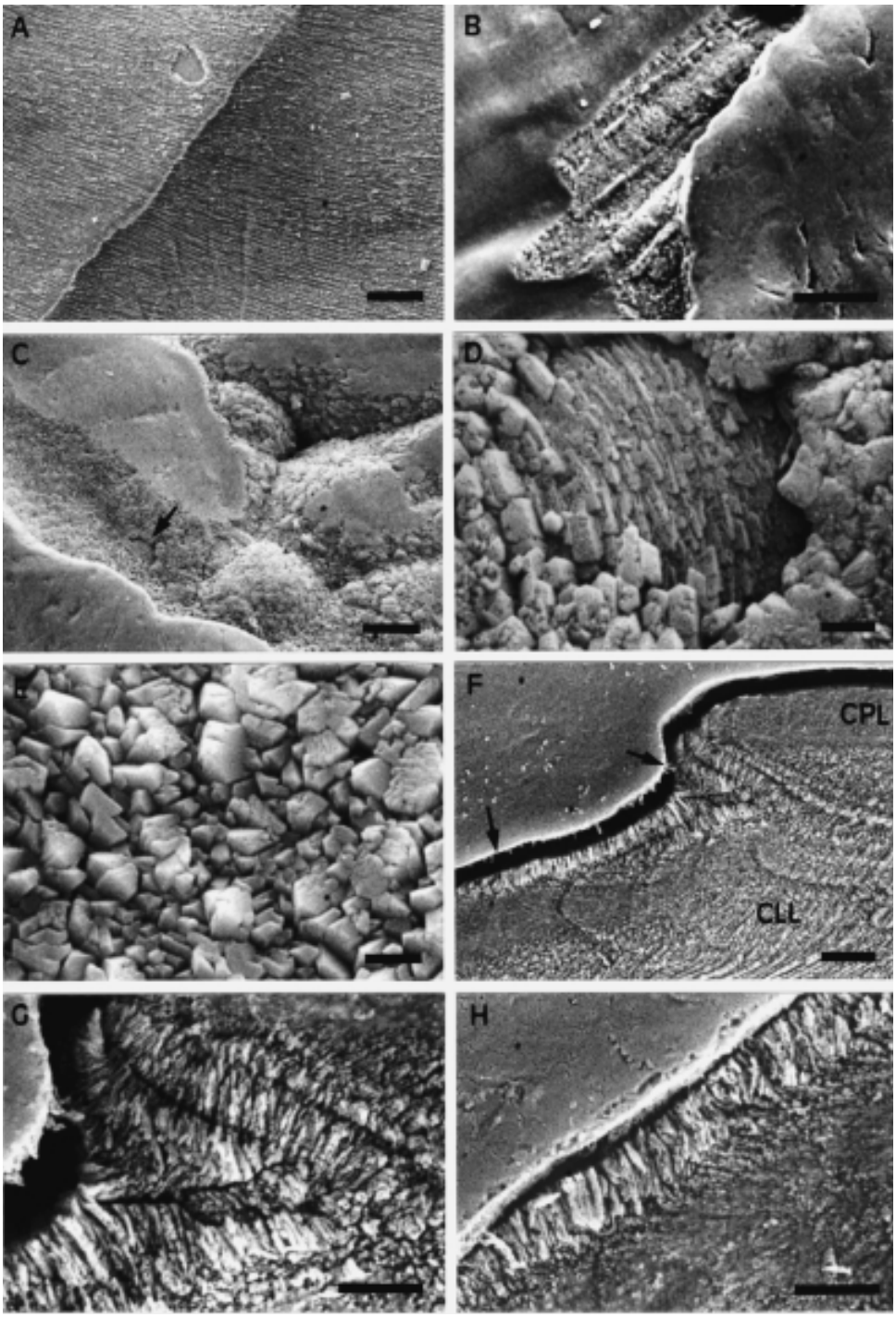
A
B
C
D
E
F
CPL
CLL
G
H

Figure 2. *Solecurtus strigilatus* (**A, C, D, E, F, G, H**) and *S. philippinensis* (**B**). **A.** SPUG.BV.142, Almería, Spain; the periostracum adapts smoothly to the rib step, thus leaving a hollow space below; wrinkles are periostracal growth lines; posterior direction to the right; scale bar = 100 μm. **B.** MNCN.15.07/4768, Luzón, Philippines; oblique view of a rib showing the area which was not lined by the periostracum; FGPs develop in this area, giving the shell surface a rougher appearance; posterior direction to the bottom left; scale bar = 50 μm. **C.** SPUG.BV.145, Almería, Spain; as in **B**, the periostracum was originally attached to the smoother areas; the boundaries between composite prisms of the outer shell layer did not grow fast enough to reach the periostracum inner surface and remained in low relief, to be later lined by FGPs; posterior direction to the top left; scale bar = 20 μm. **D.** Detail of **C** (arrow), showing a composite prism overgrown by FGPs; these are larger than the fibres of the underlying prism; scale bar = 2 μm. **E.** Detail of **C** (arrow) showing the aspect of FGPs along a rib step; ventral direction to the left; scale bar = 10 μm. **G, H.** Details of **F** (arrows); there is a change in orientation from the axes of fibres of the composite prisms to FGP axes; scale bars = 5 μm. Abbreviations: CLL, crossed-lamellar layer; CPL, composite-prismatic layer.

well preserved FGPs display well-defined pseudo-hexagonal shapes, sometimes interlocked, provided by the twinning of three aragonite prisms (Fig. 3C). The intersection of (001) crystal faces with the twinning planes of prisms (forming angles close to 60°) is evident in upper view (Fig. 3B, C). This pattern is typical of aragonite and is not found in calcite (J.M. García-Ruiz, personal communication). The loose texture of prisms makes them prone to dissolutional microboring by cyanobacteria (Fig. 3F). Results of Feigl's test reinforce the interpretation that FGPs are aragonitic.

INFERRED MODE OF FORMATION OF FREE GROWING PRISMS

In *S. strigilatus* the periostracum does not adapt to every rib scarp, but stretches smoothly across and reattaches well beyond the point in the vertical of the rib peak, leaving a gap in between (Fig. 2A, B, C). This is the place where the described crystals grow. It is unlikely that this feature is largely influenced by contraction of the periostracum due to drying. Despite the lack of extensive periostracal remains in *Strigilla*, we interpret that, as in *Solecurtus*, the periostracum did not adapt exactly to the steep posterior side of ribs.

In both genera, and in tellinoideans in general, the shell margin reflects outwards, such that the growth front of the outer shell layer is more or less transversal to the outer shell surface and, hence, to the periostracum. Composite prisms of the outer layer are parallel to the outer shell surface and their fibres radiate from their main axes (Figs. 2F, H & 3C). Those fibres radiating both outwards and forwards end at the inner surface of the periostracum. Therefore, unlike unionids (on which current models of bivalve shell formation have been established; see, e.g., Petit, David, Jones & Hagler, 1980; Saleuddin and Petit, 1983) the periostracum is not the substrate for biocalcification. Since the periostracum is secreted at the periostracal fold, at a certain distance from the (shell-secreting) margin of the outer mantle lobe (Fig. 4), it may not reproduce exactly the shape of the shell margin and thus may not adapt tightly to the shell's outer surface. The steps corresponding to ribs are present only at the very mantle margin, but vanish progressively towards the bottom of the periostracal groove. In the case of *Strigilla*, this feature could be enhanced by the fact that the mantle lobe has to extend drastically to reflect over the shell, this being particularly true for the steep side of ribs which are secreted by angular mantle extensions (Fig. 3E).

In *Solecurtus* and *Strigilla*, when we consider only the shell directly deposited by the mantle, the steep side of a given rib has a concave profile (Fig. 2G). Thus, before FGP deposition there are sinuses below the periostracum, along the posterior sides of ribs.

The irregular development of FGPs indicates that the growth surface of crystals is free and unconstrained by the presence of a mantle or inner periostracal surface. That they are not deposited by the mantle is evident also from their texture (coarser than the rest of the shell; Figs. 2D, F & 3H) and, in *Solecurtus*, from their different orientation than the fibres forming the composite prisms (Fig. 2H). The conclusion is that they grow at the interstices left between the concave surfaces of the rib steps and the periostracum (Fig. 4). Since they may reach the very margin of the shell, they have to form shortly after the mantle secreted that part of the shell. Some radial grooves in *S. polyaulax*, which are lined with FGPs can be interpreted as radial tension wrinkles developed on the

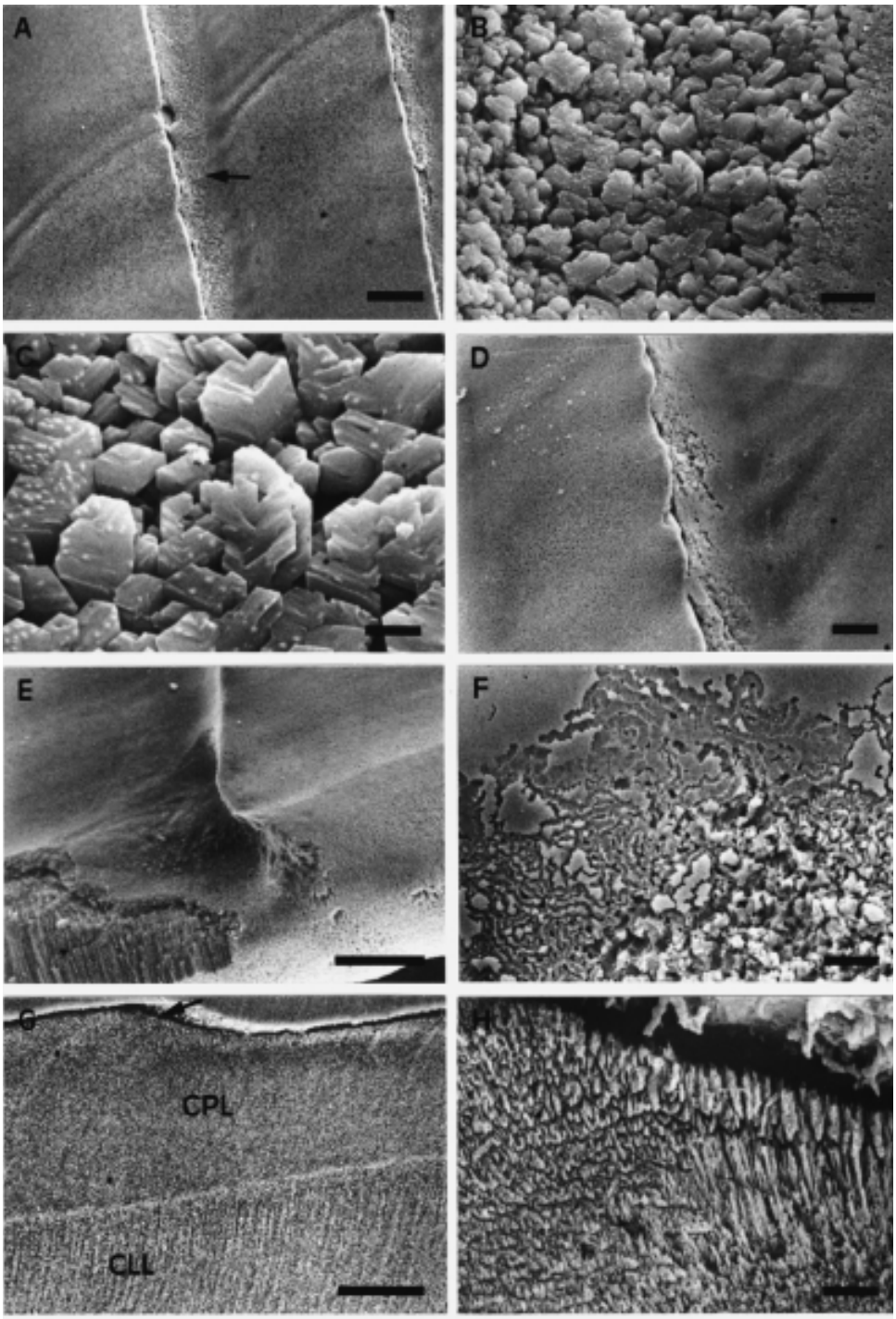
A
B
C
D
E
F
G
CPL
CLL
H

Figure 3. *Strigilla polyaulax* (**A, C, D, E, G, H**) and *S. pisiformis* (**B, F**). **A.** SPUG.BV.202, Pointe Noire, Congo Brazzaville; FGPs develop systematically at the posterior slope of ribs; posterior direction to the top right; scale bar = 50 μm. **B.** Detail of **A** (arrow) showing the aspect of FGPs and the transition to mantle-deposited shell surface; scale bar = 5 μm. **C.** Detail of **B**; pseudo-hexagonal prisms of aragonite result from the twinning of three rhombic prisms; note the even orientation of crystals; scale bar = 2 μm. **D.** MNHN, unreg., Caribbean; radial grooves lined with FGPs can be interpreted as high-relief tension wrinkles which developed in the periostracum and which were not internally filled by mantle-deposited shell; posterior direction to the upper right; scale bar = 20 μm. **E.** Same specimen as in **A** (right valve); view of the valve margin showing the most distal position reached by the mantle margin during shell secretion; there were angular extensions of the outer mantle lobe which attached at the posterior side of each rib (see also Fig. 4); scale bar = 50 μm. **F.** MNHN, unreg., Caribbean; cyanobacterial microborings develop exclusively on FGPs, and not on the rest of the shell; posterior direction towards the top; scale bar = 10 μm. **G.** SPUG.BV.203, Pointe Noire, Congo Brazzaville; polished radial section showing arrangement of shell layers and FGPs; growth lines indicate strong reflection of the mantle during shell deposition; ventral direction to the left; scale bar = 50 μm. **H.** Detail of **G** (arrow), showing alignment of FGPs with fibres of composite prisms; scale bar = 5 μm. Abbreviations: CLL, crossed-lamellar layer; CPL, composite-prismatic layer.

periostracum which were not originally filled with mantle deposits (Fig. 3D).

Whether the mantle is extended during calcification periods or contracted, it is consistently found at the distal ends of the channels formed as described above (Fig. 4). Therefore, it can be assumed that during the bivalve's life these sinuses would still have been filled with extrapallial fluid (at least for a short time), provided that the periostracum is well preserved. FGPs can grow within these spaces, since, given its composition, the extrapallial fluid is a medium especially suitable for calcium carbonate deposition (Crenshaw, 1972, 1990; Wada & Fukinuki, 1976; Wilbur & Saleuddin, 1983). FGPs can be classified as remote biominerals since their deposition takes place without contact with the mantle, although directly influenced by the fluids deriving from it. Crystal growth proceeds by epitaxy, on the substrate provided by fibres of composite prisms, as evidenced by the fact that FGPs grow as a continuation of fibres and are evenly oriented (Fig. 3C). The change in orientation recorded in *Solecurtus* (see above) comes from the need of FGPs to grow perpendicular to the substrate in their mutual competition for space.

Alternatively, FGPs can be interpreted as early marine cements formed during the bivalve's life where the outer shell surface is directly exposed to sea water and, in particular on the posterior rib slopes. This interpretation is not supported here, since in the forms examined the periostracum has been largely lost, being preserved only at a certain distance from the margin. No particular FGPs, outside the posterior rib sides, have been found associated with these areas.

As commented above, other species do not develop FGPs associated with their divaricate ribs (Table 1). In the light of the above model of formation, this absence is understandable for several reasons. In *Solecurtus* and *Strigilla*, voids between the calcified shell and the periostracum are formed because the steep sides of the ribs are more or less concave before FGP deposition, and the periostracum spreads flat across. In the species reportedly lacking FGPs, this is never the case. In *Acila* (Fig. 5A) and *Myllita* there is little difference in slope between the two gentle sides of ribs. In *Digitaria* it can easily be seen that the periostracum adapts tightly to ribs, which are quadrate in profile and have vertical sides (Fig. 5B). In the remaining genera, ribs are more (*Divaricella, Divalucina*; Fig. 5C) or less (*Gari*; Fig. 5D) markedly asymmetric, but the steep sides of ribs are neither vertical nor concave. In addition, FGPs are not present in the posterior area of the *Strigilla* shell, where ribs have more symmetric profiles. In conclusion, divaricate ribs of *Solecurtus* and *Strigilla* are unique in their profile. The question remains as to whether the periostracum is the substrate for shell deposition in some of the species mentioned, which would prevent local detachment from the shell.

FINAL REMARKS

FGPs are described here for the first time in bivalves. These deposits are aragonitic simple prismatic in microstructural terms. The major difference from the equivalent normal shell microstructure in bivalves is the free crystalline endings of prisms. FGPs resemble inorganic crystals in that their growth front was not limited at any time by the surface of the mantle. They are, therefore, reminiscent of some calcereous skeletons on which the organic phase

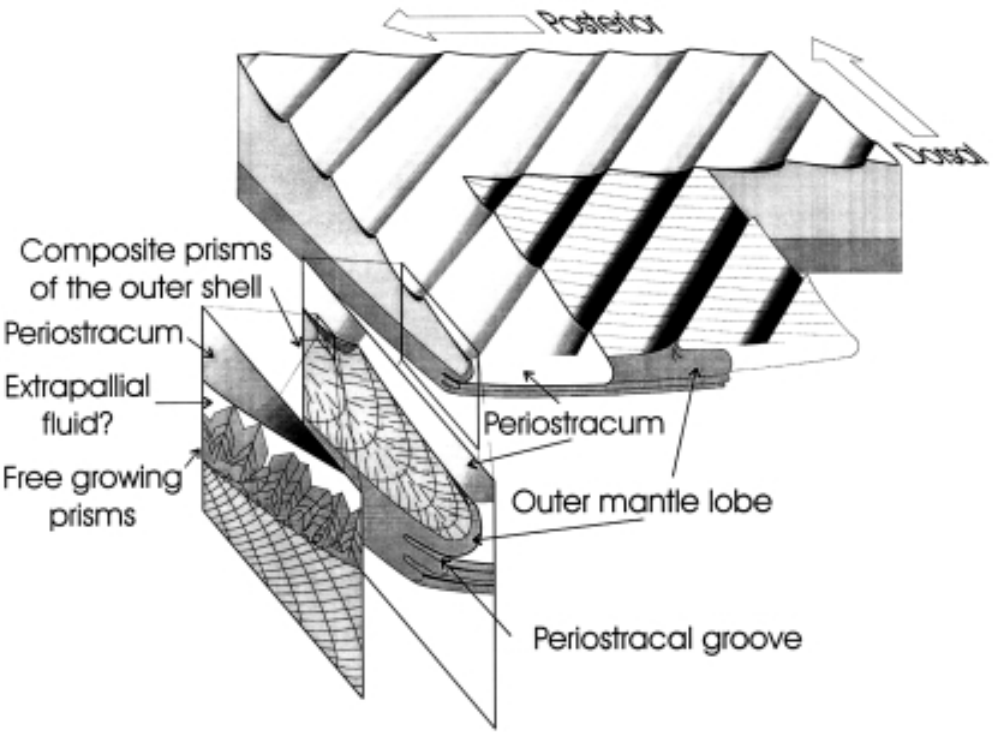

Figure 4. Model for the formation of free-growing prisms, as exemplified in *Strigilla*. The periostracum detaches from the outer shell at the posterior (steeper) side of ribs and, if well preserved, it can prevent sea water from flooding the spaces thus formed, which remain filled with extrapallial fluid. Aragonite prisms (FGPs) form within these microenvironments. They grow epitaxially onto the fibres of the composite prisms of the outer shell (insets).

exerts little control and which are largely dominated by physicochemical processes (Lowenstam, 1981; Constantz, 1986; Harper, 1992). Since they appear to have grown within the extrapallial fluid, but not in contact with the mantle, they constitute a case of remote biomineralization, and the only one reported in bivalves which is aragonitic. Within Mollusca, Kemperman & Gittenberger (1988) found aragonite crystals, usually arranged into sheets, within the hollow ribs of the pulmonate clausiliid *Albinaria*. Unlike bivalve FGPs, crystals in *Albinaria* have unevenly oriented crystallographic axes. They are probably formed on the surface of droplets of extrapallial fluid trapped within the internal spaces of ribs. This case is presently under study.

From the constructional standpoint, FGPs are what Seilacher (1973) termed 'fabricational noise', that is, by-products of the very process of fabrication, which allows one to make morphogenetic inferences. FGPs probably have no adaptive value. On the contrary, they flatten an otherwise concave rib profile, which would probably be more effective in gripping sediment grains to prevent backward slippage when the foot probes into the sediment during burrowing. This implies that the bivalve mode of shell formation poses limits for the profiles of divaricate ribs.

ACKNOWLEDGEMENTS

Thanks are given to Dr. J.M. García-Ruiz (Laboratorio de Estudios Cristalográficos, CSIC-Univ. Granada) for his advise concerning crystal growth. Prof. S. Gofás (Muséum National d'Histoire Naturelle, Paris), and Dr. J. Templado (Museo Nacional de Ciencias Naturales, Madrid) kindly selected and provided material on loan from their institutions. Profs. C. Salas (Universidad de Málaga, Spain) and R. Schmidt-Effing (Philipps Universität Marburg, Germany) yielded material of *Digitaria digitaria* and *Divaricella quadrisulcata*, respectively. Drs E.M. Harper (Cam-

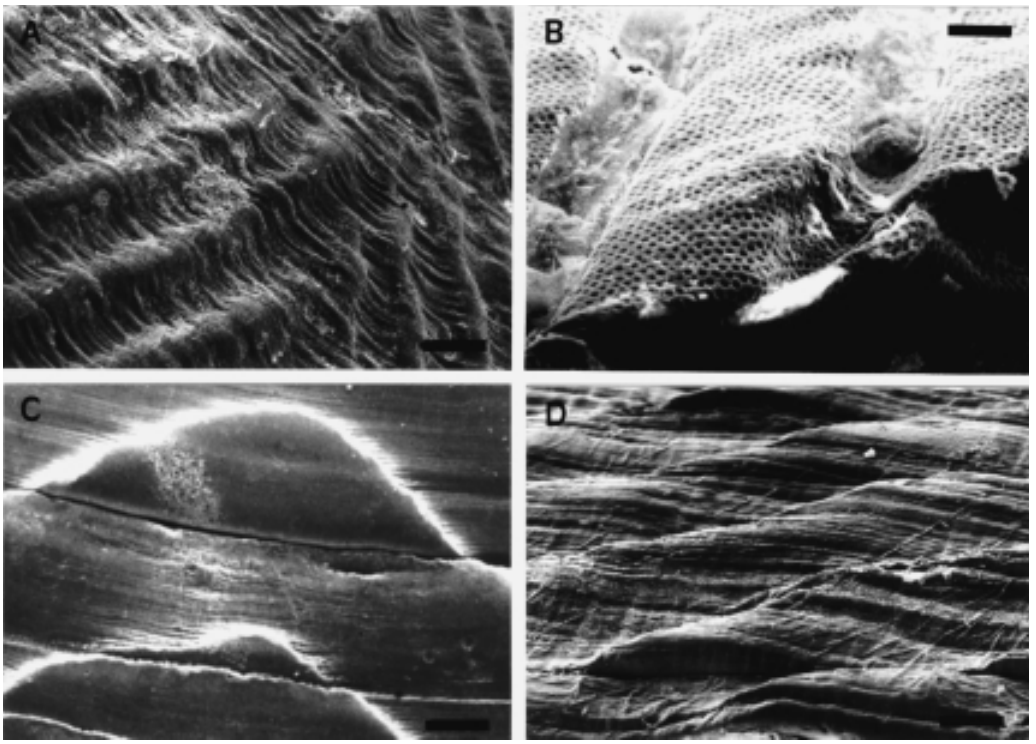

Figure 5. A. *Acila* sp. (MNHN. unreg.), Philippines; oblique view of left valve showing divaricate ornament; scale bar = 200 μm. **B.** *Digitaria digitaria* (SPUG.BV.63), Málaga, Spain; view of the ventral area, showing the profile of ribs; anterior direction to the left; scale bar = 50 μm. **C.** *Divaricella quadrisulcata* (SPUG.BV.94), Isla Mujeres, México; divaricate ribs of the central area of a right valve; scale bar = 200 μm. **D.** *Gari squamosa* (MNCN.15.07/0142), Philippines; oblique view of the margin of a right valve showing profile of oblique ribs; scale bar = 200 μm.

bridge University) and J.D. Taylor (The Natural History Museum, London) suggested significant improvements of the manuscript. This study has been financed by project PB97-0790 of the DGESIC (Ministerio de Educación y Cultura) and by the Research Group RNM 0178 (Junta de Andalucía).

REFERENCES

CHINZEI, K. & SEILACHER, A. 1993. Remote biomineralization. I: Fill skeletons in vesicular oyster shells. *Neues Jahrbuch für Geologie und Paläontologie Abhandlungen*, **190**: 349-361.

CONSTANTZ, B.R. 1986. Coral skeleton construction: a physicochemically dominated process. *Palaios*, **1**: 152-157.

CRENSHAW, M.A. 1972. The inorganic composition of the molluscan extrapallial fluid. *Biological Bulletin*, **143**: 506-512.

CRENSHAW, M.A. 1980. Mechanisms of shell formation and dissolution. In: *Skeletal growth of aquatic organisms: biological records of environmental change* (D.C. Rhoads & R.A. Lutz, eds), 115-132. Plenum Press, New York.

CRENSHAW, M.A. 1990. Chapter 1. Biomineralization mechanisms. In: *Skeletal biomineralization: patterns, processes and evolutionary trends, 1* (J.G. Carter, ed.), 1-9 Van Nostrand Reinhold, New York.

FEIGL, F. 1937. *Qualitative analysis by spot test*. Nordemann Publications Company, New York.

HARPER, E.M. 1992. Post-larval cementation in the Ostreidae and its implications for other cementing Bivalvia. *Journal of Molluscan Studies*, **58**: 37-48.

KEMPERMAN, TH.C.M. & GITTENBERGER, E. 1988. On morphology, function and taxonomic importance of the shell ribs in Clausiliidae (Mollusca: Gastropoda Pulmonata), with special reference to those in *Albinaria. Basteria*, **52**: 77-100.

LOWENSTAM, H.A. 1981. Minerals formed by organisms. *Science*, **211**: 1126-1131.

LOWENSTAM, H.A. & WEINER, S. 1989. *On biomineralization*. Oxford University Press, Oxford.

PETIT, H., DAVIS, W.L., JONES, R.G. & HAGLER, H.K. 1980. Morphological studies on the calcification

process in the fresh-water mussel *Amblema. Tissue & Cell*, **12**: 13-28.

SALEUDDIN, A.S.M. & PETIT, H. 1983. The mode of formation and the structure of the periostracum. In: *The Mollusca*, **4**: *Physiology, Part 1* (A.S.M. Saleuddin & K.M. Wilbur, eds), 199-234. Academic Press, New York.

SEILACHER, A. 1972. Divaricate patterns in pelecypod shells. *Lethaia*, **5**: 325-343.

SEILACHER, A. 1973. Fabricational noise in adaptive morphology. *Systematic Zoology*, **22**: 451-465.

SEILACHER, K. & CHINZEI, A. 1993. Remote Biomineralization. II: Fill skeletons controlling buoyancy in shelled cephalopods. *Neues Jahrbuch für Geologie und Paläontologie Abhandlungen*, **190**: 363-373.

STANLEY, S.M. 1970. Relation of shell form to life habits of the Bivalvia (Mollusca). *Geological Society of America Memoir*, **125**: 1-296.

TAYLOR, J.D., KENNEDY, W.J. & HALL, A. 1973. The shell structure and mineralogy of the Bivalvia. II. Lucinacea-Clavagellacea. Conclusions. *Bulletin of the British Museum (Natural History), Zoology*, **22**: 256-294.

WADA, K. & FUJINUKI, T. 1976. Biomineralization in bivalve molluscs with emphasis on the chemical composition of the extrapallial fluid. In: *The mechanisms of mineralization in animals and plants* (N. Watabe & K.M. Wilbur, eds), 175-190. University of South Carolina Press, Columbia.

WILBUR, K.M. & SALEUDDIN, A.S.M. 1983. Shell formation. In: *The Mollusca*, **4**: *Physiology, Part 1* (A.S.M. Saleuddin & K.M. Wilbur, eds), 235-287. Academic Press, New York.